2010

Application of the Marsupial Paradigm to Tropical Cyclone Formation from Northwestward Propagating Disturbances

Zhuo Wang, Timothy J. Dunkerton

Application of the Marsupial Paradigm to Tropical Cyclone Formation from Northwestward-Propagating Disturbances

ZHUO WANG

Department of Atmospheric Sciences, University of Illinois at Urbana–Champaign, Urbana, Illinois

TIMOTHY J. DUNKERTON

NorthWest Research Associates, Bellevue, Washington, and Naval Postgraduate School, Monterey, California

MICHAEL T. MONTGOMERY

Naval Postgraduate School, Monterey, California

(Manuscript received 24 August 2010, in final form 31 January 2011)

ABSTRACT

A wave-tracking algorithm is developed for northwestward-propagating waves that, on occasion, play a role in tropical cyclogenesis over the western oceans. To obtain the Lagrangian flow structure, the frame of reference is translated obliquely at the same propagation speed with the precursor disturbance. Trajectory analysis suggests that streamlines in the obliquely translated frame of reference can be used to approximate flow trajectories. The algorithm was applied to Super Typhoon Nakri (2008), Tropical Cyclone Erika (2009), and a few other examples. Diagnoses of meteorological analyses and satellite-derived moisture and precipitation fields show that the marsupial framework for tropical cyclogenesis in tropical easterly waves is relevant also for northwestward-propagating disturbances as are commonly observed in the tropical western Atlantic, the Gulf of Mexico, and the western North Pacific. Finally, it is suggested that analysis of the global model data and satellite observations in the marsupial framework can provide useful guidance on early tropical cyclone advisories.

1. Introduction

Dunkerton et al. (2009, hereafter DMW09) recently proposed a new model for tropical cyclone formation within the critical layer of a tropical easterly wave. Through a survey of 55 named storms over the Atlantic and east Pacific during 1998–2001, they showed that the critical layer of an easterly wave is important to tropical storm formation, and that the intersection of the trough axis and the critical surface of the wave—the center of the cat's eye in the wave critical layer—is the preferred location for tropical cyclone formation. The conceptual framework for this multiscale process is regarded as a ''marsupial paradigm'' in which a protovortex is carried along by the parent synoptic-scale wave until it is strengthened into an incipient tropical cyclone, or ''tropical depression.'' The cat's eye within the wave critical layer can also be called the wave's ''gyre pouch'' insofar as it represents a quasi-closed region of recirculating horizontal flow protected from hostile exterior influences (i.e., dry air intrusion and shear/strain deformation). Recirculation of lower-tropospheric flow in the comoving frame is a necessary but not sufficient condition for tropical cyclone formation in tropical easterly waves (DMW09).

Through high-resolution real-case and idealized numerical simulations, respectively, Wang et al. (2010a,b) and Montgomery et al. (2010a) demonstrated that the meso-α motion in the cat's eye of the synoptic-scale wave critical layer provides a focal point for the merger of vortical convective structures and their vortical remnants, and that a tropical storm forms close to the center of the wave's gyre pouch via system-scale convergence in the lower troposphere and vorticity aggregation.

Based on the marsupial framework, Wang et al. (2009) proposed a real-time forecast method for tropical easterly

Corresponding author address: Zhuo Wang, Department of Atmospheric Sciences, University of Illinois at Urbana–Champaign, Urbana, IL 61801.
E-mail: zhuowang@illinois.edu

DOI: 10.1175/2011MWR3604.1

waves in the Atlantic and eastern Pacific basins to predict the track of the possible genesis locations within these wave disturbances using global model operational data. They showed that as a region of approximately closed Lagrangian circulation, the easterly wave's gyre pouch, when it exists, is characterized by a distinct moisture gradient ahead of the wave trough, which separates the relatively moist air within from the relatively dry air outside the pouch. The moisture gradient propagates westward with the wave, and the propagation speed of the pouch can be estimated based on a Hovmöller diagram of the moisture front.[1] Wang et al. (2009) showed that the genesis location of a tropical storm can be predicted using global model forecast data up to three days in advance with less than 1° error when and if genesis occurs. A similar method is also found to apply to easterly waves over the western North Pacific, and the diagnosis of the global model data in the marsupial framework provided useful guidance in flight planning during the Tropical Cyclone Structure 2008 (TCS-08) field experiment (Montgomery et al. 2010b) and during the Pre-Depression Investigation of Cloud Systems in the Tropics (PREDICT) field experiment in 2010 (Montgomery et al. 2012).

Observational support for the marsupial framework thus far has been obtained mainly for tropical easterly waves, which play an important role in tropical cyclone formation over the Atlantic and the eastern-central Pacific. As their name implies, easterly waves propagate from east to west with a predominantly zonal component of phase propagation. Over the western North Pacific, the large-scale circulation is more complicated because of the prominent monsoon circulation, and tropical cyclone formation is found to be associated with different synoptic-scale patterns (e.g., Ritchie and Holland 1999; Lander 1994; Harr et al. 1996; Fu et al. 2007; Montgomery et al. 2010b). Such patterns generally represent a superposition of quasi-stationary mean-flow structures (e.g., ITCZ, monsoon trough, equatorial depression, etc.) with propagating transients riding on or alongside these structures. Besides tropical easterly waves and westward-moving equatorially trapped waves (Molinari 2004), tropical cyclones in the western Pacific may also form in association with (i) tropical depression (TD) disturbances (e.g., Liebmann and Hendon 1990; Lau and Lau 1990; Takayabu and Nitta 1993; Dunkerton 1993; Frank and Roundy 2006) and (ii) disturbances excited by Rossby wave dispersion from a preexisting tropical cyclone (e.g., Frank 1982; Davidson and Hendon 1989; Briegel and Frank 1997). Unlike tropical easterly waves or equatorial waves, these disturbances propagate northwestward with a meridional component of phase propagation that is comparable to, or greater than, the zonal component.

Such meridional propagation is not limited to the western North Pacific. Easterly waves often turn northward over the western North Atlantic and the Gulf of Mexico, instead of following a zonal path.[2] The method proposed in Wang et al. (2009) is no longer applicable when the meridional propagation speed of the precursor disturbance is not negligible compared to the zonal propagation. However, the marsupial framework (DMW09) does not preclude meridional phase propagation, although the choice of comoving frame is simplest when the wave propagation is quasi-monochromatic, irrespective of horizontal direction.

This study offers an alternative wave-tracking technique to the Hovmöller-based methods, which is useful also for zonally propagating waves, and it extends the real-time forecast algorithm developed in Wang et al. (2009) to obliquely propagating disturbances. (Here we refer to the northwestward direction as ''oblique'' with respect to the equator and other latitude circles.) Super Typhoon Nakri (2008) over the western North Pacific, Tropical Storm Erika (2009) over the western Atlantic, and a few other examples are used to show that the marsupial paradigm also applies to tropical cyclone formation from northwestward-propagating disturbances.

The data used in this study are described in section 2. The wave-tracking method and the oblique translation are presented in section 3. The illustrative examples are

[1] It is necessary to point out a subtle difference between tracking a moisture *front* at the edge of the cat's eye and a moisture (or vorticity) *maximum* within. Propagation of the moist front is equivalent to propagation of the quasi-closed Lagrangian circulation structure in the wave critical layer. However, *pouch-relative motion* (cyclonic circulation associated with the wave) during cat's-eye rollup projects on the apparent propagation speed when tracking vorticity or moisture maxima. The apparent propagation (of maxima) represents the sum of the actual propagation of the wave and a pouch-relative cyclonic component which, for westward waves, adds to (subtracts from) the westward component poleward (equatorward) of the critical surface (Dunkerton 1991; see Fig. 1 of DMW09). This relative motion is responsible for cyclonic homogenization of vorticity and moisture inside the gyre pouch and introduces an unnecessary complication in the determination of pouch propagation speed.

[2] Deviation from westward propagation occurs for a variety of reasons: wave refraction on the zonally varying mean flow, a fracture or split of the original trough line, and the generation of a secondary easterly wave. Not surprisingly, there are instances in the Northern Hemisphere when the northern part of the wave becomes the locus of tropical cyclone formation while the southern part continues to propagate westward.

shown in section 4. Section 5 presents a summary of the main results of this study.

2. Data

Global Forecast System (GFS) 6-hourly, 1° × 1° analyses are used in this study to depict the evolution of the precursor disturbances: their synoptic-scale structure, propagation, and meso-α kinematic and dynamical features. Similar to Wang et al. (2009), the raw GFS data are used, and no temporal filters are applied. The same diagnoses can be done using global model operational data [such as the European Centre for Medium-Range Weather Forecasts (ECMWF), GFS, the Navy Operational Global Atmospheric Prediction System (NOGAPS), or the Met Office (UKMO) forecasts] for real-time forecasts. Besides the GFS analysis data, total precipitable water (TPW) from the Cooperative Institute for Meteorological Satellite Studies (CIMSS) and the Tropical Rainfall Measuring Mission (TRMM) 3B42 3-hourly accumulated precipitation from the National Aeronautics and Space Administration (NASA) are also used to examine the moisture content and convective activity within the wave gyre pouch. The former is the morphed integrated microwave imagery (MIMIC) obtained by combining disparate swaths of satellite observations using a data-blending technique (Wimmers and Velden 2007), and the latter has the resolution of 0.25° × 0.25°.

3. Wave tracking for northwestward-propagating waves

a. Vorticity centroid tracking

A vorticity centroid tracking method is proposed for horizontally propagating waves. For a wave's gyre pouch, the vorticity centroid $(\overline{x}, \overline{y})$ is defined as

$$\overline{x} = \frac{\sum\limits_{\text{gyre}} x_i \zeta_i}{\sum\limits_{\text{gyre}} \zeta_i} \quad \text{and} \quad \overline{y} = \frac{\sum\limits_{\text{gyre}} y_i \zeta_i}{\sum\limits_{\text{gyre}} \zeta_i}, \tag{1}$$

where the subscript i denotes grid points within the pouch. According to DMW09, the boundary of the gyre pouch can be approximately defined as the bounding streamfunction contour, which depends on the parent wave's propagation velocity. Since the velocity vector is not known a priori, we calculate the vorticity centroid for an 8° × 8° box as the first step of an iterative procedure. The initial location of the box is selected subjectively based on the distribution of vorticity, and the subsequent location of the box center is specified to match the vorticity centroid obtained in the previous time step. The size of the box is designed to capture all of the relevant vorticity and is large enough to ensure that most or all of this vorticity stays in the same box after one time step. In this way, the first-guess box moves with the wave's gyre pouch and its associated cyclonic vorticity as time progresses. To reduce the uncertainties that might be introduced by the initial box location at the first step, the vorticity centroid tracking is done backward in time, starting from a strong disturbance or a tropical storm with a coherent vorticity structure (in a real-time forecast, 5-day forecasts can be used for backward tracking). The zonal and meridional propagation speeds of the pouch are then derived from the centroid track using a 3-day linear regression, which reduces the high-frequency variations in the pouch track due to the interaction between the wave pouch and mesoscale processes.[3] The second step of the iteration is as follows. Using this propagation speed, a translated streamfunction is constructed, and the pouch boundary is then approximated by the value of the translated streamfunction intersecting the saddle point on the separatrix, usually the saddle point nearest the pouch center (DMW09). A second iteration is then performed to determine the vorticity centroid more accurately and objectively based on this approximate pouch boundary, encompassing only the relevant vorticity and nothing more (or less); a 2D propagation velocity of the pouch is then derived from this updated centroid track based on a 3-day linear regression. This 2D velocity is then used to translate the frame of reference.

At the early stage of the wave, the vorticity field may be disorganized and the vorticity centroid may differ from the gyre-pouch center, which depends on the initial distribution of vorticity and wrap-up of the vorticity within the pouch. As vorticity becomes consolidated around the gyre-pouch center, the vorticity centroid is usually close to the gyre-pouch center (DMW09). Thus, the vorticity centroid track can be used as an approximation of the gyre-pouch track to derive the wave's propagation speed and direction. Both tracking methods are superior to tracking of individual vorticity maxima, as vorticity maxima are manifestation of meso-β vortices (the "joeys") within the gyre pouch, which are subject to high-frequency variations and pouch-relative motions in the cat's-eye circulation as diagnosed in the comoving frame. The cyclonic swirling motion of transient vortex

[3] The high-frequency variations of the pouch track may also be due to the temporal inconsistence of the GFS data.

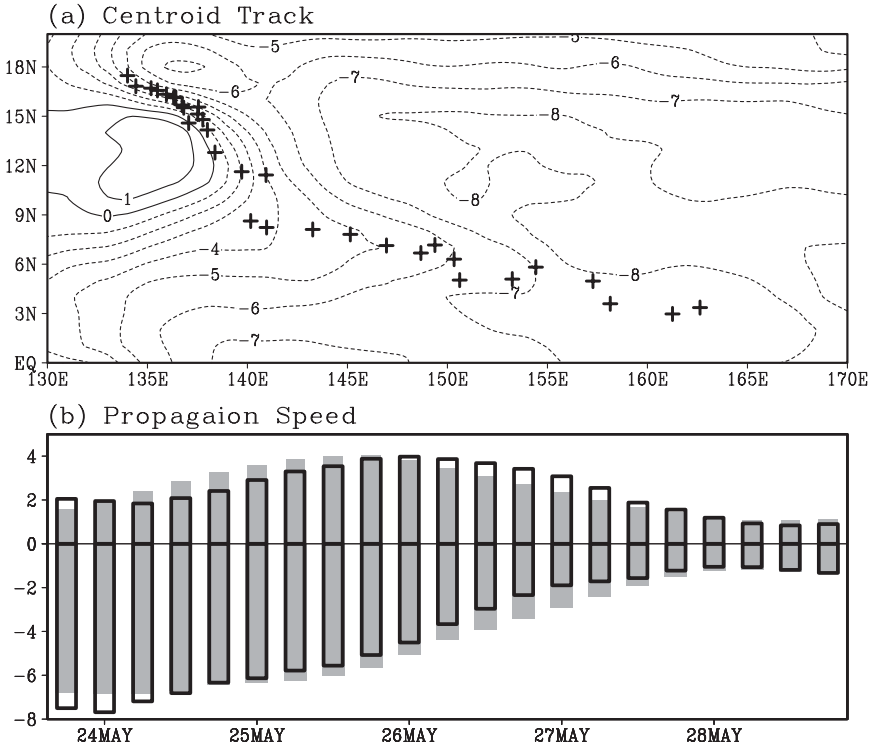

FIG. 1. (a) The vorticity centroid track of the pre-Nakri gyre pouch during 0600 UTC 22 May–0600 UTC 30 May superimposed on zonal wind averaged over the same time period, and (b) the zonal (negative values) and meridional (positive values) components of the propagation speed of the vorticity centroid derived for an 8° × 8° box (gray bars) and for the pre-Nakri gyre pouch (thick black bars). The time interval of the pouch track in (a) is 12 h. The abscissa in (b) is speed in m s^{-1}.

joeys can be visualized in the so-called Fujita diagram (Wang et al. 2010b; Montgomery et al. 2010a) showing the rotation of individual protovortex elements about the gyre-pouch center, where the tropical depression eventually forms. By contrast, the moisture front (Wang et al. 2009) and vorticity centroid represent a bulk property of the wave's gyre pouch largely independent of the vorticity "microstructure" within the pouch [i.e., vortical hot towers (VHTs) and mesoscale convective vortices (MCV)] and the coarse-grained overturning of the critical layer itself (Fig. 1 of DMW09). For zonally propagating easterly waves, the pouch tracks that are determined individually from translated streamlines and vorticity centroid usually agree well (not shown).

According to the Joint Typhoon Warning Center (JTWC), Nakri developed into a tropical depression at 1400 UTC 27 May 2008. In this study we will focus on the time period prior to the formation of the tropical depression, 21–27 May. The vorticity centroid is first derived for an 8° × 8° box and then for the wave's gyre pouch as described earlier in this section (Fig. 1). At the early stage (1800 UTC 21 May–0600 UTC 24 May), the disturbance resembles a mixed Rossby–gravity wave (MRG) pattern, with a westward-propagating, counterclockwise circulation centered at the equator (in the moving frame). A faster-propagating, weak easterly wave along 8°N merges with the MRG-type disturbance on 23 May, and this seems to help enhance the circulation. After 24 May, the disturbance resembled a TD-type disturbance: it propagates northwestward and is followed by a ridge to its southeast. The evolution of the disturbance is consistent with Takayabu and Nitta (1993) and Dunkerton and Baldwin (1995), which showed the transition of MRG disturbances to TD-type disturbances from the central Pacific to the tropical western North Pacific.

Figure 1b shows the propagation speeds of the pouch track. Both zonal and meridional components change in time, and the wave propagation slows down as the genesis time approaches. This is probably due to the change of the mean flow and the enhanced moist convection within the wave pouch. In this case, the propagation speed derived for the 8° × 8° box and that derived for the wave's gyre pouch differ by less than 1 m s^{-1}.

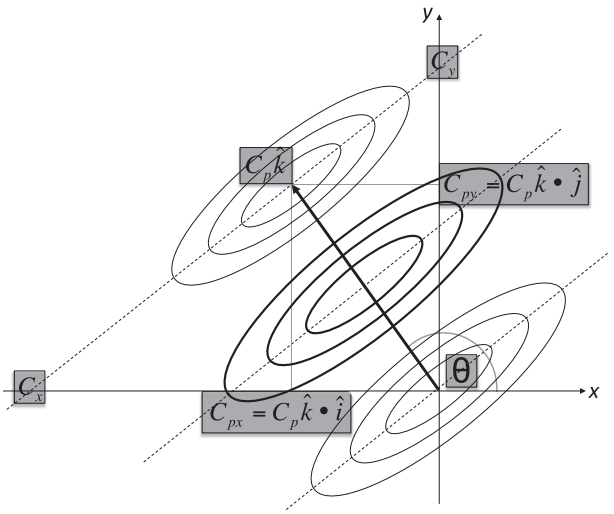

FIG. 2. A schematic showing the wave propagation speed. The thick and thin contours represent positive and negative perturbations associated with a wave, and the dashed lines represent the constant phase lines, where $\hat{\mathbf{k}}$ is the unit wave vector, C_p is the propagation speed in the wave propagation direction, and C_{px} and C_{py} are the zonal and meridional propagation speeds, respectively, of the vorticity centroid. The variables C_x and C_y are the apparent speeds of wave propagation in the x and y directions, respectively, which are larger than C_p and satisfy $C_x \cdot C_{\mathrm{px}} = C_y \cdot C_{\mathrm{py}}$; θ is the angle between the wave propagation direction and the x axis.

b. *Oblique translation and the preferred genesis location*

For zonally propagating waves, the preferred genesis location or gyre-pouch center is determined by the intersection of the critical surface and the trough axis of the parent wave. The critical latitude is defined as $u - C_p = 0$, and the trough axis is defined as $v = 0$ and relative vorticity is cyclonic (DMW09), where u and v are the zonal and meridional components of the wind, respectively. Therefore, in the frame of reference that translates zonally at the propagation speed C_p, the gyre-pouch center is a stagnation point with zero flow. This can be generalized for two-dimensionally (2D) propagating waves as follows.

First, the frame of reference will be translated in the direction of the wave propagation and at the same propagation speed. Assume the zonal and meridional propagation speeds of the vorticity centroid are C_{px} and C_{py}, respectively, then the angle between the wave propagation direction and the horizontal direction can be determined as

$$\theta = \arccos\left(C_{\mathrm{px}} \Big/ \sqrt{C_{\mathrm{px}}^2 + C_{\mathrm{px}}^2}\right), \tag{2}$$

where $\theta = 90°$ for northward propagation and $\theta = 180°$ for westward propagation.

Propagation speed in the wave propagation direction is

$$C_p = \sqrt{C_{\mathrm{px}}^2 + C_{\mathrm{py}}^2}. \tag{3}$$

Note that here C_{px} and C_{py} are the zonal and meridional propagation speeds, respectively, of the vorticity centroid. As shown in the schematic (Fig. 2) the apparent speeds of wave propagation in the x and y directions (C_x and C_y, respectively) are larger than C_p. If one estimates the propagation speed based on a Hovmöller diagram along the wave propagation direction, any error in the estimated wave propagation direction may result in overestimation of the phase speed.

In the translated frame of reference, the velocity field becomes

$$\mathbf{V}' = \mathbf{V} - C_p\hat{\mathbf{k}}$$

or

$$\begin{cases} u' = u - C_{\mathrm{px}} \\ v' = v - C_{\mathrm{py}} \end{cases}, \tag{4}$$

where $\hat{\mathbf{k}}$ is the unit wave vector, and a prime denotes the wave-relative flow or the flow in the translated frame. Note that since the translation speed may not be a constant, the coordinates are noninertial coordinates. This adds an apparent force on the system, but the apparent force does not introduce any torque in the vorticity budget equation. Besides, vorticity is a Galilean invariant and does not change with the translation of the frame.

The critical latitude for 2D propagating waves is defined as where the wave-relative flow is zero in the direction of the wave propagation:

$$\hat{\mathbf{k}} \cdot (\mathbf{V} - C_p\hat{\mathbf{k}}) = 0 \tag{5a}$$

or

$$(u\cos\theta + v\sin\theta) - C_p = 0. \tag{5b}$$

The "trough axis" should then be modified as

$$\hat{\mathbf{n}} \cdot (\mathbf{V} - C_p\hat{\mathbf{k}}) = 0 \tag{6a}$$

or

$$u\sin\theta - v\cos\theta = 0, \tag{6b}$$

where $\hat{\mathbf{n}}$ is the unit vector perpendicular to the wave propagation direction. Equations (6a) and (6b) imply

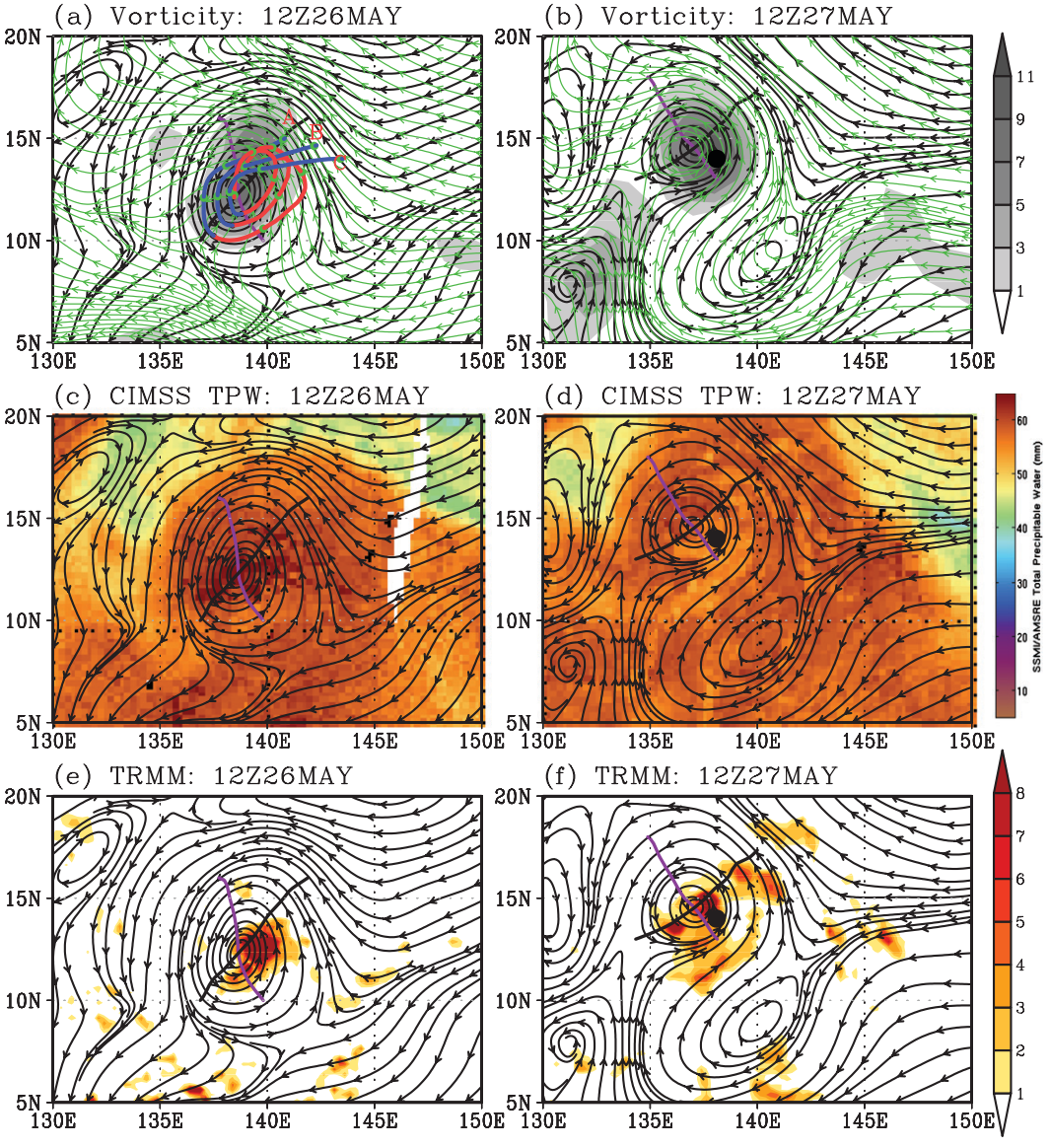

FIG. 3. (top) Relative vorticity (10^{-5} s^{-1}), (middle) CIMSS TPW (mm), and (bottom) TRMM 3B42 rain rate (mm h^{-1}) superimposed on 850-hPa streamlines (black streamlines) in the frame of reference moving obliquely at the same speed with the wave at (left) 1200 UTC 26 May (day −1) and (right) 1200 UTC 27 May (day 0). The thick black curve represents the modified wave trough axis, and the thick purple curve represents the wave critical surface. (a),(b) Green streamlines are in the earth-relative frame; A, B, and C label the trajectories of three air particles in (a). (b),(d),(f) The black dot represents the genesis location.

that the relative flow in the direction perpendicular to the wave propagation direction is zero along the modified trough axis. Therefore, the total relative flow is zero at the intersection of the critical surface and the modified trough axis, which is the wave's gyre-pouch center and the preferred location for tropical cyclogenesis in tropical waves. Note that C_p as defined in Eq. (3) is always positive. For purely westward-propagating waves, $\theta = 180°$ and Eqs. (5b) and (6b) are simplified to $u = -C_p$ and $v = 0$, respectively.

4. Illustrative examples

a. Pre-Nakri 2008

Figure 3a shows the 850-hPa streamlines and relative vorticity for the pre-Nakri disturbance at 1200 UTC 26 May (day −1) in the resting frame of reference (green streamlines) and the moving frame of reference (black streamlines), respectively. Streamlines in the earth-relative frame do not reveal the closed cyclonic

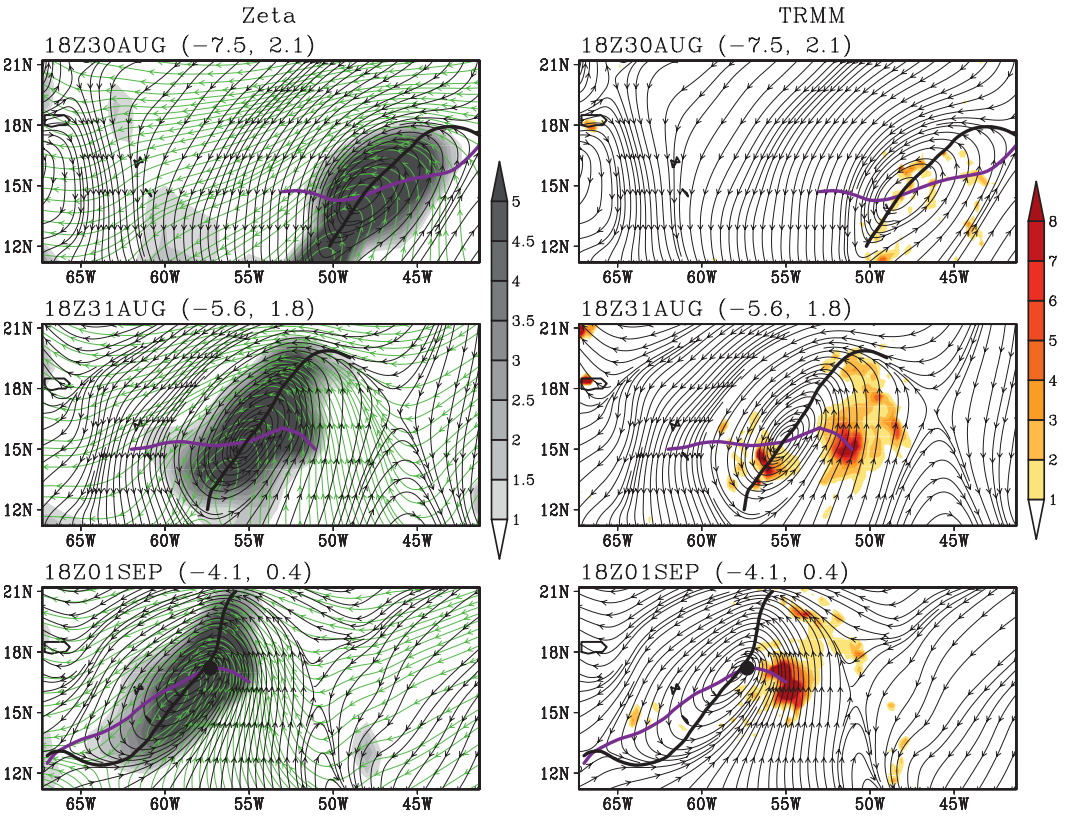

FIG. 4. (left) Relative vorticity (10^{-5} s^{-1}) and (right) TRMM precipitation rate (mm h^{-1}) superimposed on 925-hPa streamlines (black streamlines) in the frame of reference moving obliquely at the same speed with the pre-Erika disturbance at (top) 1800 UTC 30 Aug, (middle) 1800 UTC 31 Aug, and (bottom) 1800 UTC 1 Sep. (left) Green streamlines are in the earth-relative frame. The thick black curve represents the wave trough axis, and the thick purple curve indicates the local critical latitude (CL) of the wave. Erika was not declared as a tropical storm by the NHC until 2100 UTC 1 Sep 2009 because of the absence of a closed circulation near the surface. The zonal and meridional propagation speeds of the vorticity centroid (C_{px}, C_{py}) are indicated for each time in the top left of each panel.

(or anticyclonic) circulations, similar to the situation for Tropical Storm Erika as described below. The disturbance has a northeast–southwest tilt, and strong cyclonic vorticity is located in the northeastern part of the wave circulation. In the moving frame of reference, a well-defined closed circulation is present, and the center of the closed circulation is pinpointed by the intersection of the wave trough axis (black curve) and the wave critical surface (purple curve). The distribution of relative vorticity agrees much better with the translated streamlines: the strong cyclonic vorticity is largely confined within the closed circulation (the wave's gyre pouch) in the comoving frame, but displaced from the circulation center in the earth-relative frame.

To see how well the translated streamlines may represent the flow trajectories, 36-h forward (red) and backward (blue) trajectories of three air parcels within the closed circulation are shown in Fig. 3a. Because of the unsteadiness of the flow, there are discrepancies between the translated streamlines and the parcel trajectories. Nevertheless, the parcel trajectories show that there is a closed Lagrangian circulation similar to what is depicted by the translated streamlines, in contrast with the open wave pattern in the earth-relative frame. The parcel trajectories suggest that the recirculation time is about two days, which is consistent with the relative vorticity in the order of 10^{-4} s^{-1}.

One day later (day 0), the wave's gyre pouch moved to around (14°N, 137°E), and its horizontal size is reduced. An anticyclonic cell appears to the southeast of the cyclonic wave cell, which is probably due to Rossby wave energy dispersion from the storm. Genesis occurs close to the pouch center. Although a closed circulation is also present in the earth-relative frame of reference at the genesis time (not shown), the center of the circulation is

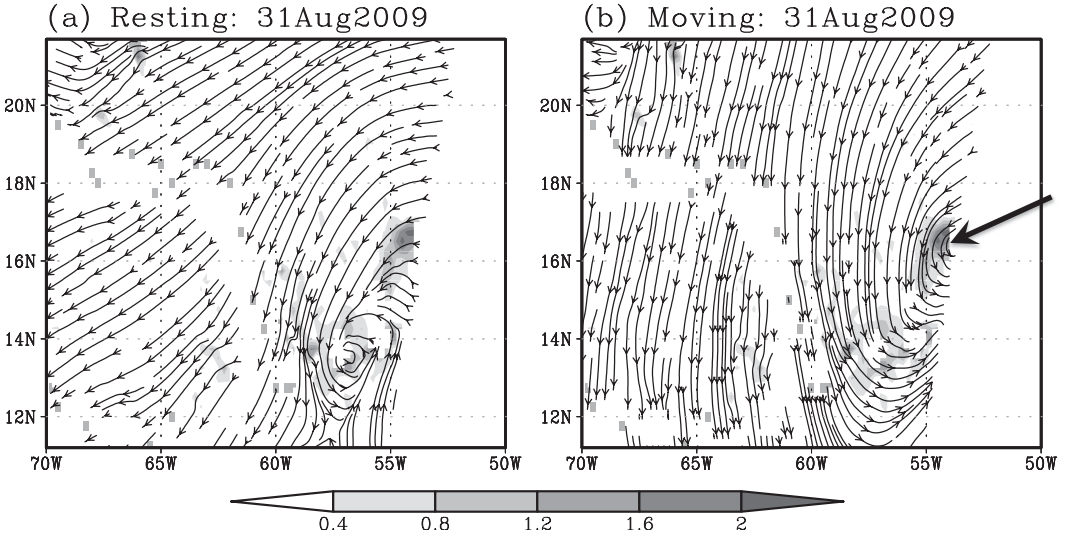

FIG. 5. Streamlines of surface flow from QuikSCAT on 31 Aug for the pre-Erika disturbance: (a) resting frame, (b) comoving frame [the same phase speeds as in Fig. 4 (middle) are used]. Shading represents relative vorticity (10^{-4} s^{-1}), and the arrow highlights the gyre-pouch center as shown in the comoving frame, which is near the edge of the QuikSCAT swath.

about 1° to the southwest of the pouch center or about 2° away from the genesis location.

To examine the moisture distribution and convective activity, MIMIC-TPW from the CIMSS and TRMM rain rate are superimposed on the translated streamlines (the middle and bottom panels in Fig. 3). Figure 3c shows that the wave's gyre pouch has abundant moisture on day −1. The northern and western boundaries of the moist air mass are consistent with the translated streamlines. Since moisture is treated as a conservative tracer in MIMIC-TPW, this suggests that the streamlines in this obliquely translated frame are a good approximation of the flow trajectories, and that this depiction of the wave's gyre pouch captures the moisture gradient on its northern and western boundaries. TRMM precipitation (Fig. 3e) shows that organized convection is located to the east of the wave trough (or in the downshear-left quadrant) and near the pouch center. The moist air mass and convection moved northwestward with the wave pattern (Figs. 3d,f). This is consistent with Takayabu and Nitta (1993), who found that convection propagates northwestward and keeps the phase relationship with the low-level circulation in a TD-type disturbance. By contrast, the MRG-type of disturbances over the equatorial central Pacific are only loosely coupled with convection. Nitta (1972) and Lau and Lau (1990) suggested that diabatic heating associated with convective activities contributes to the maintenance of TD-type disturbances. Figure 3f also shows that convection on day 0 was more extensive with a larger area of the wave pouch receiving precipitation stronger than 1 mm h^{-1} compared to day −1.

The above diagnoses show that genesis of Nakri occurred near the center of the moist, convectively active gyre pouch, and suggest that the marsupial framework can also apply to tropical depression disturbances over the western North Pacific.

b. Pre-Erika 2009

Tropical Storm Erika in 2009 is illustrated here as another example (Fig. 4). Erika originated from a tropical easterly wave over the Atlantic. The wave had a nearly zonal path over the eastern and central Atlantic, but turned northwestward west of 50°W. According to the Tropical Cyclone Report from the National Hurricane Center, the system produced deep convection continuously on 30–31 August and also had "winds to around tropical storm strength." However, it was not declared as a tropical depression until late on 1 September because it lacked a well-defined low-level center of circulation (or a well-defined closed circulation) in the earth-relative frame. Around 1800 UTC 1 September, a U.S. Air Force Reserve reconnaissance aircraft found a broad closed circulation, and the system was then classified as a tropical cyclone. If viewed in the wave comoving frame of reference, a well-defined low-level (925 hPa) closed circulation with abundant moisture and strong cyclonic relative vorticity had formed more than 2 days before the disturbance was declared as a tropical storm (Fig. 4), which is in contrast to the open-wave pattern in the resting

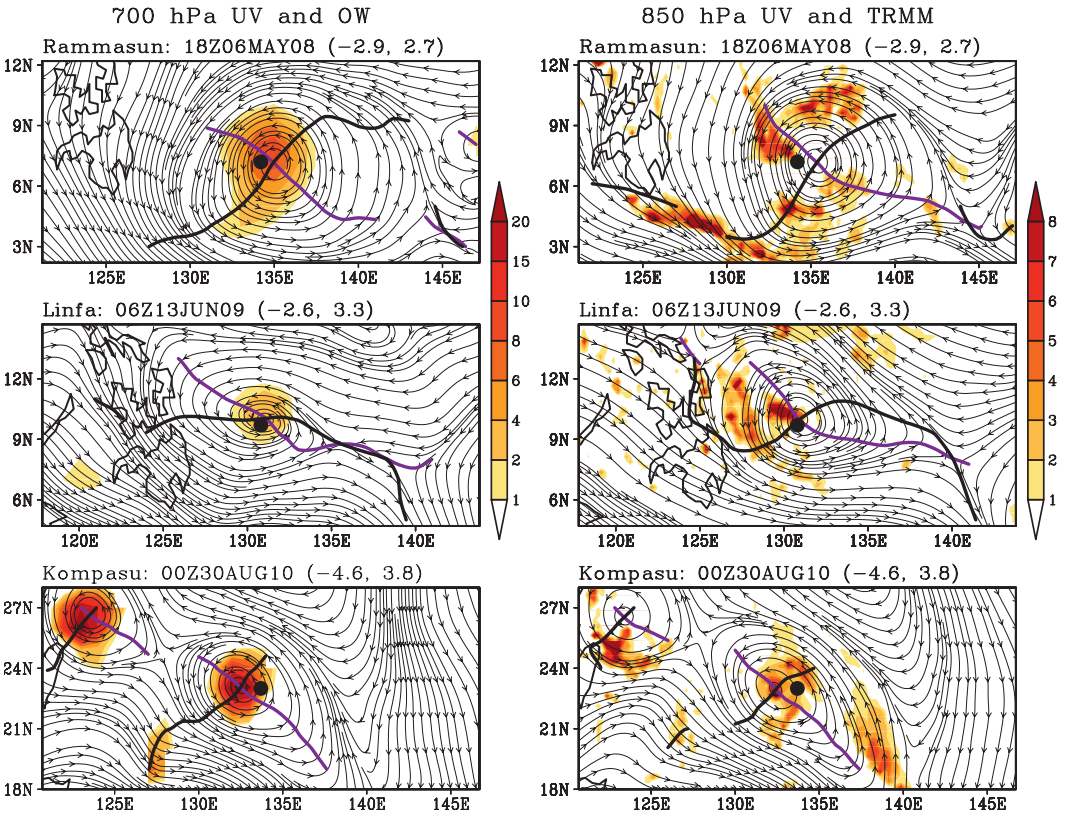

FIG. 6. (left) The OW parameter (700 hPa; 10^{-9} s^{-2}) and (right) TRMM precipitation (mm h^{-1}) superimposed on the translated streamlines at the genesis time for (top) Rammasun (2008), (middle) Linfa (2009), and (bottom) Kompasu (2010). The streamlines are at (left) 700 hPa and (right) 850 hPa. The black dot indicates the genesis location. The thick black curve represents the wave trough axis, and the thick purple curve indicates the local critical latitude (CL) of the wave. The genesis time and the zonal and meridional propagation speeds (C_{px}, C_{py}) are indicated on the top of each panel. The cyclone northwest of Kompasu is pre-Namtheun, which was upgraded to a tropical depression at 0600 UTC 30 Aug.

frame of reference.[4] TRMM data shows also that convection becomes organized east of the trough axis. The presence of a closed circulation at the surface in the wave comoving frame of reference on day −1 is also confirmed in Quick Scatterometer (QuikSCAT) data, as shown in Fig. 5. Similar to the GFS analysis (Fig. 4), QuikSCAT shows a better-defined closed circulation in the comoving frame of reference and that the gyre-pouch center is to the northeast of the circulation center in the resting frame of reference. The maximum surface relative vorticity is located near the gyre-pouch center and is about 2×10^{-4} s^{-1}. The maximum surface wind is about 14 m s^{-1} in the wave comoving frame (the maximum surface wind speed exceeds 20 m s^{-1} in the resting frame due to the contribution by the background mean flow), which suggests that the disturbance may have reached the tropical depression intensity on 31 August.

Besides Nakri and Erika, we have applied the oblique translation algorithm to the precursor disturbances of Rammasun (2008), Linfa (2009), and Kompasu (2010) over the western North Pacific and some nondeveloping waves over the Atlantic in 2008. Figure 6 shows the Okubo–Weiss (OW) parameter and TRMM precipitation rate at the genesis time of these storms. The OW parameter is defined as $\mathrm{OW} = \varsigma^2 - S_1^2 - S_2^2 = (v_x - u_y)^2 - (u_x - v_y)^2 - (v_x + u_y)^2$. Positive values of OW indicate that the flow is vorticity dominant and immune from the enstrophy cascade whereas negative values of OW indicate a strain-rate-dominant flow susceptible to rapid filamentation (McWilliams 1984). Our

[4] GFS analysis shows a small closed circulation at 925 hPa in the resting frame of reference at 1800 UTC 1 September, but the center of the circulation is about 350 km away from the genesis location, and the wave was open at 850 and 700 hPa. Note also that the meridional propagation speed is negligible at the genesis time, but a consideration of the meridional propagation at the early stage more clearly reveals the Lagrangian flow pattern.

findings from these cases indicate that (i) the wave pouch of a northwestward-propagating disturbance is a region of strong rotation and weak deformation, (ii) the pouch has high moisture content compared to the surrounding environment (not shown in Fig. 6), and (iii) convection becomes organized within the pouch, and a tropical storm forms near the center of each respective wave pouch. Our diagnoses therefore suggest that the marsupial framework can be applied to tropical cyclone formation from northwestward-propagating disturbances.

5. Summary

In this study we developed a wave-tracking algorithm and an oblique frame translation method for northwestward-propagating disturbances. The ''northwestward-propagating disturbances'' include (i) tropical easterly waves that turn northwestward over the west Atlantic, (ii) tropical depression disturbances, and (iii) wave trains related to preexisting tropical cyclones. These disturbances are known to play a role in tropical cyclogenesis over the western oceans. The wave-tracking algorithm is based on the vorticity centroid, which can capture both the zonal and meridional propagations of the disturbance. To obtain an approximate Lagrangian evolution of the wave, the frame of reference is translated in the wave propagation direction at the propagation speed. The wave's critical surface is defined based on the northwestward-propagation speed, along which the relative flow in the wave propagation direction is zero. A modified definition of the wave trough axis is proposed, so that the relative flow in the direction normal to the wave propagation direction is zero along the wave trough axis. The intersection of the wave critical surface and the trough axis pinpoints the center of the wave's gyre pouch.

The wave-tracking algorithm and the oblique frame translation method were applied to the formation of Nakri (2008), Tropical storm Erika (2009), and a few other examples. An analysis of the Lagrangian trajectories for pre-Nakri suggests that the streamlines in this obliquely translated frame of reference yield a good approximation for flow trajectories. While a disturbance may not have a closed low-level circulation in the earth-relative frame of reference, a closed Lagrangian circulation may have formed as indicated by the translated streamlines. In the illustrative examples, a tropical depression developed close to the center of the closed circulation as diagnosed in the comoving frame. The findings herein suggest that the marsupial paradigm is applicable to tropical cyclones originating from northwestward-propagating disturbances and that a corresponding analysis of the global model data and satellite observations in the marsupial framework can provide useful guidance on early tropical cyclone advisory warnings for such disturbances. Although this study only presents preliminary diagnoses of a limited number of storms, the method proposed here makes possible the examination of a large sample of northwestward-propagating precursor disturbances in the marsupial framework, and a more extensive follow-up study is under way. The results of this work will be reported in due course.

Acknowledgments. This research was supported by the National Science Foundation Grants ATM-1016095, ATM-0733380, and ATM-0851554. The GFS data are from NCAR CISL Research Data Archive (RDA).

REFERENCES

Briegel, L. M., and W. M. Frank, 1997: Large-scale influences on tropical cyclogenesis in the western North Pacific. *Mon. Wea. Rev.,* **125,** 1397–1413.

Davidson, N. E., and H. H. Hendon, 1989: Downstream development in the Southern Hemisphere monsoon during FGGE/WMONEX. *Mon. Wea. Rev.,* **117,** 1458–1470.

Dunkerton, T. J., 1991: Nonlinear propagation of zonal winds in an atmosphere with Newtonian cooling and equatorial wave driving. *J. Atmos. Sci.,* **48,** 236–263.

——, 1993: Observation of 3–6-day meridional wind oscillations over the tropical Pacific, 1973–1992: Vertical structure and interannual variability. *J. Atmos. Sci.,* **50,** 3292–3307.

——, and M. P. Baldwin, 1995: Observation of 3–6-day meridional wind oscillations over the tropical Pacific, 1973–1992: Horizontal structure and propagation. *J. Atmos. Sci.,* **52,** 1585–1601.

——, M. T. Montgomery, and Z. Wang, 2009: Tropical cyclogenesis in a tropical wave critical layer: Easterly waves. *Atmos. Chem. Phys.,* **9,** 5587–5646.

Frank, W. M., 1982: Large-scale characteristics of tropical cyclones. *Mon. Wea. Rev.,* **110,** 572–586.

——, and P. E. Roundy, 2006: The role of tropical waves in tropical cyclogenesis. *Mon. Wea. Rev.,* **134,** 2397–2417.

Fu, B., T. Li, M. S. Peng, and F. Weng, 2007: Analysis of tropical cyclogenesis in the western North Pacific for 2000 and 2001. *Wea. Forecasting,* **22,** 763–780.

Harr, P. A., R. L. Elsberry, and J. C. L. Chan, 1996: Transformation of a large monsoon depression to a tropical storm during TCM–93. *Mon. Wea. Rev.,* **124,** 2625–2643.

Lander, M. A., 1994: Description of a monsoon gyre and its effects on the tropical cyclones in the western North Pacific during August 1991. *Wea. Forecasting,* **9,** 640–654.

Lau, K.-H., and N.-C. Lau, 1990: Observed structure and propagation characteristics of tropical summertime synoptic scale disturbances. *Mon. Wea. Rev.,* **118,** 1888–1913.

Liebmann, B., and H. H. Hendon, 1990: Synoptic-scale disturbances near the equator. *J. Atmos. Sci.,* **47,** 1463–1479.

McWilliams, J. C., 1984: The emergence of isolated coherent vortices in turbulent flow. *J. Fluid Mech.,* **146,** 21–43.

Molinari, J., 2004: Paradigms of tropical cyclogenesis. *Bull. Amer. Meteor. Soc.,* **85,** 662–663.

Montgomery, M. T., Z. Wang, and T. J. Dunkerton, 2010a: Coarse, intermediate and high resolution numerical simulations of the

transition of a tropical wave critical layer to a tropical storm. *Atmos. Chem. Phys.,* **10,** 10 803–10 827.

——, L. L. Lussier III, R. W. Moore, and Z. Wang, 2010b: The genesis of Typhoon Nuri as observed during the Tropical Cyclone Structure 2008 (TCS-08) field experiment—Part 1: The role of the easterly wave critical layer. *Atmos. Chem. Phys.,* **10,** 9879–9900.

——, and Coauthors, 2012: The Pre-Depression Investigation of Cloud Systems in the Tropics (PREDICT) Experiment: Scientific basis, new analysis tools, and some first results. *Bull. Amer. Meteor. Soc.,* in press.

Nitta, T., 1972: Energy budget of wave disturbances over the Marshall Islands during the years of 1956 and 1958. *J. Meteor. Soc. Japan,* **50,** 71–84.

Ritchie, E. A., and G. J. Holland, 1999: Large-scale patterns associated with tropical cyclogenesis in the western Pacific. *Mon. Wea. Rev.,* **121,** 2027–2043.

Takayabu, Y. N., and T. Nitta, 1993: 3–5 day-period disturbances coupled with convection over the tropical Pacific Ocean. *J. Meteor. Soc. Japan,* **71,** 221–246.

Wang, Z., M. T. Montgomery, and T. J. Dunkerton, 2009: A dynamically-based method for forecasting tropical cyclogenesis location in the Atlantic sector using global model products. *Geophys. Res. Lett.,* **36,** L03801, doi:10.1029/2008GL035586.

——, ——, and ——, 2010a: Genesis of pre-Hurricane Felix (2007). Part I: The role of the wave critical layer. *J. Atmos. Sci.,* **67,** 1711–1729.

——, ——, and ——, 2010b: Genesis of pre-Hurricane Felix (2007). Part II: Warm core formation, precipitation evolution, and predictability. *J. Atmos. Sci.,* **67,** 1730–1744.

Wimmers, A. J., and C. S. Velden, 2007: MIMIC: A new approach to visualizing satellite microwave imagery of tropical cyclones. *Bull. Amer. Meteor. Soc.,* **88,** 1187–1196.